PCCP

PAPER

View Article Online
View Journal | View Issue

Cite this: *Phys. Chem. Chem. Phys.*, 2016, **18**, 21760

Received 7th June 2016,
Accepted 13th July 2016

DOI: 10.1039/c6cp03940e

www.rsc.org/pccp

Selective gas capture *via* kinetic trapping†

Joyjit Kundu,* Tod Pascal, David Prendergast and Stephen Whitelam*

Conventional approaches to the capture of CO_2 by metal–organic frameworks focus on equilibrium conditions, and frameworks that contain little CO_2 in equilibrium are often rejected as carbon-capture materials. Here we use a statistical mechanical model, parameterized by quantum mechanical data, to suggest that metal–organic frameworks can be used to separate CO_2 from a typical flue gas mixture when used under nonequilibrium conditions. The origin of this selectivity is an emergent gas-separation mechanism that results from the acquisition by different gas types of different mobilities within a crowded framework. The resulting distribution of gas types within the framework is in general spatially and dynamically heterogeneous. Our results suggest that relaxing the requirement of equilibrium can substantially increase the parameter space of conditions and materials for which selective gas capture can be effected.

1 Introduction

The burning of carbon-based fossil fuels and the consequent release of CO_2 into the atmosphere causes climate change.[1] One technology designed to remove CO_2 from the flue (exhaust) gases of power plants is based upon metal–organic frameworks (MOFs), modular crystalline materials whose internal binding sites can host gas molecules.[2–11] Standard approaches to understanding gas capture in MOFs focus on equilibrium conditions,[6,12–18] where the prescription for selective gas capture is both simple and restrictive: in equilibrium, a framework will harbor CO_2 in preference to the other gas types in a mixture if the framework binds more strongly to CO_2 than to all the other gas types. For many frameworks, and for flue gas mixtures, this is not the case.[18] For instance, Mg-MOF-74 is a framework commonly used in the laboratory for gas capture.[5,8,9,14,19–21] When exposed to CO_2 mixed with H_2O, which is abundant in flue gases, Mg-MOF-74 will, under equilibrium conditions, contain mostly H_2O.[15,22–24] One response to this problem is to design a material, such as diamine-appended MOF-74,[15,16] better able to capture CO_2 in equilibrium. Another response, explored in this paper, is to consider the possibility of doing gas capture under nonequilibrium conditions.

Gas capture is a dynamic phenomenon.[22–25] Exposed to a MOF, a collection of gas molecules will execute various microscopic processes, including moving through the open space of the framework, and binding to and unbinding from it. In the long-time limit the fraction of a certain gas type resident within the framework is determined by the set of molecule-framework binding affinities, but at intermediate times the composition of gas types within the framework depends in addition on the kinetic parameters that govern the rates of molecular processes.[21,24–28] Quantum mechanical calculations[22] suggest that some frameworks not useful for selective gas capture under equilibrium conditions might perform the same task well under nonequilibrium conditions. For instance, the binding enthalpies of the flue–gas constituents H_2, CO_2, and H_2O in Mg-MOF-74 at $T = 298$ K are -0.16 eV, -0.49 eV, and -0.75 eV, respectively.[20,22] Thus, when exposed to a typical flue–gas mixture (12–15% CO_2 and 5–7% H_2O[29]), we would expect in equilibrium that most of Mg-MOF-74's binding sites will harbor water molecules (recall that eV $\approx 39 k_B T$ at 298 K). This expectation is consistent with experiment.[15,24] However, quantum mechanical calculations also indicate that different gas types do not diffuse equally rapidly within the framework. MOF-74 is a three-dimensional structure within which run quasi-one-dimensional channels. Guest molecules binding to open metal sites 'coat' the interiors of these channels and restrict the flow of gases through them. In order to move one unit cell down a channel 'coated' with molecules of its own kind, a molecule of H_2, CO_2, or H_2O feels an energy barrier of 0.005 eV, 0.04 eV, or 0.06 eV, respectively.[22] Thus one might expect H_2 to invade the framework first, followed by CO_2, followed by H_2O, with each gas eventually displacing the previous one because of its larger binding affinity for the framework. In this scenario, CO_2 could in principle reside within the framework for some time period in a quantity that exceeds its (negligible) equilibrium abundance.

Here we use a statistical mechanical model of gas diffusion and binding within a model framework to confirm this expectation: for a set of three gas types whose hierarchy of (emergent)

Molecular Foundry, Lawrence Berkeley National Laboratory, Berkeley, CA 94720, USA. E-mail: jkundu@lbl.gov, swhitelam@lbl.gov

† Electronic supplementary information (ESI) available. See DOI: 10.1039/c6cp03940e

mobilities is the reverse of their hierarchy of binding affinities, as for H_2, CO_2, and H_2O in Mg-MOF-74 (this hierarchy of affinities and mobilities is widely observed in many porous materials, *e.g.* zeolites[30] and other MOFs[18,19,31]), a gas that is essentially absent from the framework under equilibrium conditions can be captured under nonequilibrium conditions. The origin of this selective capture is an emergent nonequilibrium 'filtration' mechanism that allows, within a crowded framework, certain gas types to invade more rapidly than others. We describe this gas separation mechanism and show that the residence time and the abundance of the desired gas can be increased by impeding the flow of all gases within the framework, consistent with experiments in which constriction of pore apertures in metal–organic frameworks improved the selectivity of a framework for particular gas types.[10,32–35]

Because of the model's simplicity we do not expect it to be quantitatively precise, but where comparison can be made our results agree qualitatively with experiments,[15,24,31,32,36] and indicate that CO_2 can under nonequilibrium conditions occupy a substantial fraction of the framework's binding sites. We anticipate that doing gas capture under nonequilibrium conditions will substantially increase the space of protocols and materials for which selective gas capture can be effected.

2 Model and simulation details

We consider a square lattice of $L_y \times L_z$ sites, with periodic boundary conditions imposed in the y-(vertical) direction (see Fig. 1). The column $z = 0$ is held in contact with an equimolar (in Fig. S1, ESI† we show that our qualitative conclusions are unchanged if we take the relative abundance of gas types to be typical of a flue–gas mixture; see Section S1, ESI†) reservoir of H_2, CO_2, and H_2O molecules, each represented by a distinct type of particle the size of one lattice site. The boundary $z = L_z - 1$ is closed. This represents a simple model of experiments in which one face of the framework is exposed to gas, similar in that respect to the setup of a 'breakthrough experiment'. Having both ends open would allow gas invasion at approximately twice the rate, but our qualitative conclusions would be no different. A site (i,j) is called a binding site (denoted by bold circles in Fig. 1) if i and j are both even. The remaining sites are called free sites, intended to represent empty space. A site can be empty or occupied by a single particle of any type. Particles are hard, and cannot overlap. Particles at free sites do not interact with the framework; particles at binding sites possess a favorable interaction energy of −0.16 eV, −0.49 eV, or −0.75 eV if the particle represents H_2, CO_2 or H_2O, respectively.[13,20,22] Particles experience intra-species pairwise nearest-neighbor repulsive interactions of strength 0.0025 eV, 0.02 eV, or 0.03 eV for H_2, CO_2 or H_2O, respectively. We impose these interactions so that particles moving along the z-axis, past occupied binding sites, experience the energy barriers that particles in Mg-MOF-74 experience as they diffuse along the c-axis, through channels 'coated' by molecules of the same type.[22] We set inter-species nearest-neighbor interactions to be the arithmetic mean of the appropriate intra-species interactions, but we observe little change in our results upon setting inter-species interactions to zero: Fig. S1(b) (ESI†). Such robustness indicates that motion through its own species is the process that controls the invasion time of a particular gas type. We assume that all interaction energies are independent of temperature. The basic unit of length is set by the distance ($\approx$6.8 Å) between two metal sites within the same pore along the c-axis of Mg-MOF-74, corresponding to two lattice units in our model. We therefore set the lattice constant $\Delta\ell$ = 3.4 Å. As in Mg-MOF-74, H_2O binds to the framework most strongly but experiences the largest energy barriers to motion along occupied channels, and H_2 binds most weakly but experiences the smallest energy barrier to motion along occupied channels.

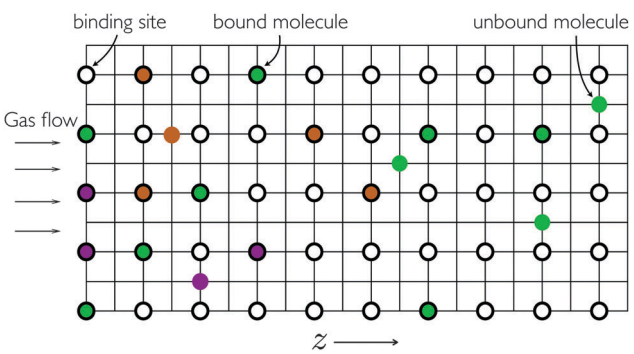

Fig. 1 Lattice model of a framework for gas capture. The leftmost column (z = 0) is in contact with a gas reservoir. Sites denoted by bold circles are binding sites. Gas molecules on binding sites receive a favorable energetic interaction. Different colors correspond to different gas types. The alternating rows running along the z-axis with no binding sites mimic the one-dimensional channels of MOF-74 along the c-axis. In this schematic the length of the framework along the z axis (L_z) is 20 lattice sites or 68 Å. Typical sizes of single crystals used in experiments range from 5–25 μm.[21]

We evolved the lattice model (Fig. 1) using a semi-grand canonical Monte Carlo algorithm that allowed single-particle insertion, removal, and diffusion processes. We considered the basic microscopic rates for insertion, removal and diffusion processes to be R_i, R_r, and R_d, respectively. The 'total rate' is defined as $R \equiv L_y R_i + n_0 R_r + n R_d$, where n_0 is the instantaneous number of particles on the first column of the lattice, and n is the instantaneous total number of particles on the lattice. With respective probabilities $L_y R_i/R$, $n_0 R_r/R$, or $n R_d/R$ we attempted an insertion, a deletion, or a diffusion move. To attempt an insertion we chose uniformly one of the L_y sites in the first column of the lattice, and attempted to place a particle on that site. The particle was chosen to be of type corresponding to H_2, CO_2, or H_2O with equal likelihood. To attempt a removal we chose uniformly any of the n_0 particles on the first column of the lattice, and proposed to remove it from the lattice. To attempt a diffusion move we chose uniformly one of the n particles on the lattice, and proposed with uniform likelihood to move that particle to any one of its four nearest-neighbor sites. We accepted each proposed move with probability

$$p_{\mathrm{acc}} = \min\left(1, \frac{R_{\mathrm{before}}}{R_{\mathrm{after}}} e^{-\beta \Delta U}\right). \quad (1)$$

This form of p_{acc} is chosen to satisfy detailed balance, ensuring equilibrium at long times (for details, see Section S1, ESI†). Here R_{before} and R_{after} are the values of the total rate R before and after the proposed move; $\beta \equiv 1/(k_B T)$; and ΔU is the energy change resulting from the proposed move. This energy change accounts for particle-framework binding enthalpies, hard-core particle site exclusions, and particle–particle nearest-neighbor interactions. For diffusion moves, in addition, any proposal to take a particle across the left or right extremity of the simulation box was rejected. For insertion and removal moves the form (1) corresponds to the choice of fixed chemical potential $\mu = -k_B T \ln(3R_r/R_i)$. For the simulations presented in the paper we set $R_r = 2$ and $R_i = 5$. After every proposed move we updated time by an amount $(R_d/R)\Delta t$, where Δt is the basic unit of time in our model. By setting $\Delta t = 10^{-10}$ s we obtain qualitative agreement with experiments that measure the equilibration time of water in a framework pre-loaded with CO_2[24] (see Section S2 and Fig. S2, ESI†). Simulation details for gas mixtures of variable composition are discussed in Section S1 (ESI†).

Simulations were begun from an empty lattice. We define the density $\rho_j(t)$ of a gas of type $j \in \{H_2, CO_2, H_2O\}$ as the fraction of binding sites occupied at time t by gas type j, averaged over many independent simulations. Particles not on binding sites do not contribute to these densities. The resulting dynamics allows particles to enter the framework from its open edge, and to diffuse within and interact with the framework. The lattice is simpler in geometrical terms than MOF-74, which is three-dimensional, but it captures the quasi-one-dimensional aspect of gas diffusion within the real structure as an emergent phenomenon: we found that dynamics was largely insensitive to the vertical extent L_y of the lattice, because motion of particles into the bulk of the framework is controlled by one-dimensional motion along 'channels' adjacent to binding sites (see Fig. S3, ESI†). In what follows we present distances and times in units of $\Delta\ell$ = 3.4 Å and $\Delta t = 10^{-10}$ s, respectively.

3 Results

CO_2 can be captured under nonequilibrium conditions

The results presented here are for an equimolar gas mixture. In Fig. 2(a) we show the time evolution of the densities of bound gas species within a single framework at 463 K where $L_z = 80$ (in units of $\Delta\ell$). All gas types are bound within the framework for some time period. The bound fractions of H_2 and CO_2 reach maxima and decline to zero, leaving water to occupy the framework at long times. Thus in equilibrium the bound fraction of CO_2 within the model framework is effectively zero, as it is in Mg-MOF-74.[15,24] However, at early times as many as half of the framework's binding sites host a CO_2 molecule, *i.e.* CO_2 can be 'captured' under nonequilibrium conditions.

Fig. 2(b) shows at three fixed times the fraction of bound gas as a function of distance z from the gas reservoir. This plot reveals the nature of the nonequilibrium gas-separation mechanism that operates within the framework. It is initially empty. At early times the columns near the reservoir become occupied

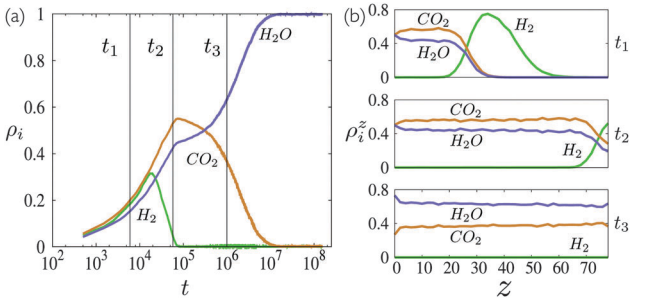

Fig. 2 Gases absent from a framework in equilibrium can be captured under nonequilibrium conditions. (a) Time evolution of the fraction of binding sites occupied by each gas type in our lattice model of a single Mg-MOF-74 crystal. (b) Fraction of binding sites in the framework occupied by each species as a function of the distance z from the gas reservoir, at three different times. Data were obtained for a lattice of size L_y = 40, L_z = 80, at 463 K, averaged over 100 independent simulations. Distances and times are reported in units of $\Delta\ell$ = 3.4 Å and $\Delta t = 10^{-10}$ s, respectively.

by an approximately random mixture of all gas types. New gas molecules must pass through these columns in order to enter the framework. As they do so, H_2O and CO_2 molecules feel a greater energy barrier to their passage than do H_2 molecules, and so the latter invade the framework fastest (upper panel). This 'filtration' effect is an emergent consequence of the energy barriers felt by particles passing through a crowded framework, which we have parameterized using quantum mechanical data.[22] Absent these barriers the gas types diffuse equally rapidly along occupied channels. The gas composition of the framework at early times is spatially heterogeneous. Eventually CO_2 and H_2O invade the framework and displace the more weakly-binding H_2 (middle panel). At long times CO_2 is displaced homogeneously by H_2O (middle and bottom panels). Eventually, H_2O occupies most of the binding sites and the framework equilibrates.

The spatial distribution of gas types within the framework depends on system size

The characteristic time for a bound molecule to unbind from an isolated binding site, which we call the unbinding time, is governed by the ratio of binding enthalpy and temperature, but the invasion time of a gas (*e.g.* the time taken to occupy 15% of the sites at the closed end of the lattice) depends both on energetic parameters and on L_z. As shown in Fig. 3(a), the invasion time τ (in units of Δt) of CO_2 scales as $L_z^{1.98}$ at 328 K and 463 K. Also shown on the plot are the characteristic unbinding times of CO_2 at those two temperatures. We see two distinct regimes. In one, the invasion time of CO_2 is larger than its unbinding time. Here we find CO_2 to be displaced by water in a spatially heterogeneous way, as shown in panel (b), because the open side of the framework approaches equilibrium while CO_2 is still invading. In the other regime, illustrated in panel (c), the invasion time of CO_2 is smaller than its unbinding time. Here CO_2 will reach the closed end of the framework without substantial CO_2 unbinding occurring, and it will subsequently be displaced by water in a spatially homogeneous way.

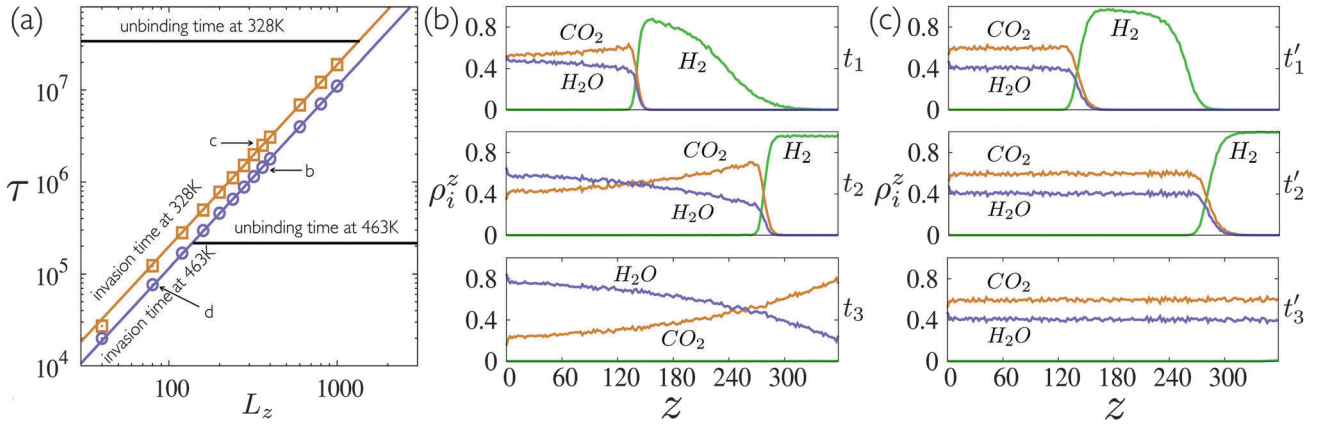

Fig. 3 (a) The invasion time of CO_2 scales with system size, but its unbinding time does not, and thus the nature of the invasion mechanism depends on system size. Simulation data (symbols) can be fit by the sloping lines, respectively $21.71L_z^{1.98}$ and $12.62L_z^{1.98}$ for 328 K and 463 K. Panels (b) and (c) show time-ordered density profiles at state points b and c on panel (a), where the invasion time of CO_2 is respectively greater than and less then its unbinding time (L_y = 40; data are averaged over 100 independent simulations). Point d on panel (a) corresponds to Fig. 2(b).

The maximum abundance ρ_{max} of bound CO_2 within the framework (at any time) also depends on L_z: it is insensitive to L_z for L_z small enough that CO_2's invasion time is smaller than its unbinding time, and diminishes with L_z for L_z large enough that CO_2's invasion time is larger than its unbinding time: see Fig. 4(a). The 'crossover' length L_c separating these two regimes depends strongly upon temperature, scaling roughly as $L_c \sim \exp(\beta E/q)$, where E is the binding enthalpy of CO_2, and $q \approx 2$ (varying weakly with T). The inset of Fig. 4(a) shows that the time at which the maximum abundance of CO_2 is attained increases as a power of L_z. Our results suggest that at 298 K, a framework with $L_z = L_c \approx 1$ μm ($\tau \approx 23.1L_z^2$) will harbor CO_2 at more than 40% of its binding sites (in Mg-MOF-74) up to a time τ_{res} (residence time) ~0.1 s (see Fig. S4, ESI†).

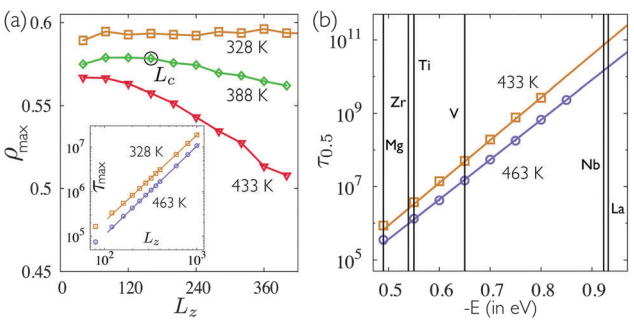

Fig. 4 (a) Maximum occupancy of CO_2 as a function of L_z at different temperatures. The label L_c indicates the 'crossover lengthscale' (at 388 K) at which invasion and unbinding times of CO_2 are comparable. Inset: Time of maximum occupancy of CO_2 as a function of the linear extent L_z of the framework at two different temperatures. The straight lines through the data for 328 K and 463 K have equations $t_{max} = 28.18L_z^{1.94}$ and $t_{max} = 10.55L_z^{2.00}$, respectively. Here L_y = 40. (b) Time at which the bound fraction of CO_2 decays to 0.5, as a function of the binding enthalpy of CO_2, at 433 K and 463 K (here L_y = 10 and L_z = 100). Straight lines are Arrhenius fits: $\tau_{0.5} = A\exp(-E/k_BT)$, where A (433 K) ≈ 1.31 and A (463 K) ≈ 1.30. The vertical lines correspond to different metals (in MOF-74) with different binding enthalpies for CO_2 (all have higher binding affinity for H_2O).[23,37] Here we fix the binding enthalpies of H_2 and H_2O to be −0.15 eV and −2.00 eV respectively.

Gas capture can be effected simultaneously for a range of system sizes

Gas capture experiments often use powders whose grain sizes are broadly distributed.[21] Nonequilibrium gas capture can occur simultaneously, in our model, for systems having a range of values of L_z, indicating that nonequilibrium gas capture can be effected in a MOF powder whose grains possess a distribution of sizes. A simple strategy to maximize gas uptake by a powder is to ensure that grains' characteristic lengths are smaller than L_c. At low temperatures, ρ_{max} decays slowly with L_z, and so there exists a range of grain sizes within which CO_2 can be captured in abundance. In Fig. S5 (ESI†), we plot the density of bound CO_2 in a framework as a function of L_z at different times and temperatures. This plot indicates that at a fixed temperature and time, an appreciable fraction of CO_2 can be bound within grains of a range of sizes. We suggest that for efficient nonequilibrium CO_2 capture one could use grains whose average size is less than L_c, arranged in a thin bed so as to allow simultaneous exposure to gas. Otherwise, different parts of the bed may equilibrate at different times, reducing the overall nonequilibrium uptake capacity.

Gas capture timescales can be made experimentally convenient

The timescale on which nonequilibrium capture can be achieved can be increased through choice of metal constituents of MOF-74 that bind CO_2 more strongly than does Mg. This is true even if those metals bind water more strongly and so are bare of CO_2 in equilibrium; thus, the requirements for gas capture out of equilibrium are less restrictive than for capture in equilibrium: see Fig. 4(b). For all the metal types presented in Fig. 4(b), H_2O has the largest binding affinity and H_2 has the lowest binding affinity for the framework. Our aim is to show the effect of varying the binding affinity of CO_2 on its residence

time within the framework. For simplicity we hold fixed the binding enthalpies of H_2 and H_2O, because neither binding affinity controls the residence time of CO_2 nearly as strongly as does CO_2's own binding affinity: the binding affinity of H_2O is larger than that of CO_2, and so H_2O will eventually displace CO_2 from the framework, but the timescale on which H_2O displaces CO_2 is not strongly dependent upon H_2O's binding affinity (as we do not consider any exchange mechanism in the model). Similarly, because the unbinding time of H_2 is small compared to that of CO_2, small variations in the binding affinity of H_2 do not strongly influence the residence time of CO_2. For instance, a single MOF-74 crystal of length 1 μm, made from a metal whose binding enthalpy with CO_2 is −0.70 eV, which is experimentally realizable, can harbor CO_2 up to a time of ∼460 s at 298 K (we obtained $\tau_{res} \approx 0.13$ s when $E = -0.49$ eV by extrapolation, thus $\tau_{res}(E = -0.70$ eV) may be estimated using the formula $\tau_{res}(E) \propto \exp[-E/k_BT]$: see Fig. 4(b)). At that temperature the crossover length, the grain size limit at which nonequilibrium uptake capacity is maximum, is $L_c \approx 59$ μm. Our results indicate that for such system sizes, the resident time of CO_2 (at 298 K) within the framework can be up to few hours.

The time 'window' of CO_2 capture can also be enlarged by increasing the separation of timescales associated with the nonequilibrium 'filtration' mechanism, which can be achieved by impeding the flow of gases into the framework. In Fig. 5 we show a density plot of CO_2 occupancy within a framework as a function of time t and temperature T. The window of nonequilibrium CO_2 capture is defined in the figure as the two contours (Arrhenius fits to the data) of 50% CO_2 occupancy; within this region more than half of all binding sites host CO_2. Fig. 5(a) represents the case in which energy barriers to motion along z-axis of the model framework for different gas types are similar to those in fully-occupied ('coated') hexagonal channels of Mg-MOF-74.[22] In Fig. 5(b) we show that a broadening of the nonequilibrium CO_2 capture window and higher CO_2 occupancy can be achieved by increasing the separation of timescales associated with diffusion events only. We have done this by multiplying all particle–particle interactions, which control the emergent energy barriers to motion in a crowded framework, by an arbitrary factor of 5, so impeding the flow of all gases into the framework. In a real framework a similar effect might be achieved by making the channels of the framework narrower. Constriction of pore apertures in metal–organic frameworks has been seen to improve the selectivity of a framework for particular gas types in experiment[10,32–35] and atomistic simulation.[38,39]

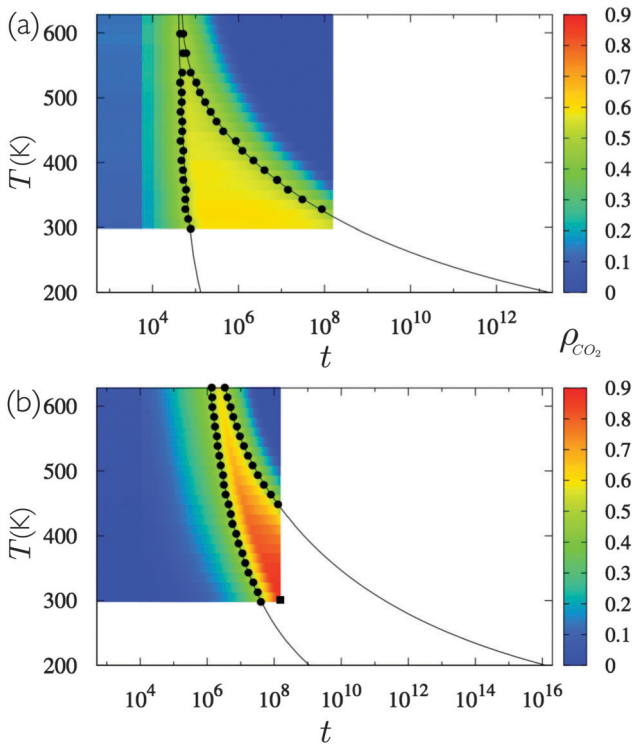

Fig. 5 The nonequilibrium CO_2 capture window can be shifted and broadened by increasing the separation of timescales of basic microscopic processes. We plot the bound CO_2 fraction, as a function of t, for simulations run at a range of temperature T. In panel (a) the values of the barriers opposing the diffusion in a crowded framework of H_2, CO_2 and H_2O molecules are taken from quantum mechanical simulations.[22] In panel (b) we have increased all barriers by an arbitrary factor of 5, in order to demonstrate that impeding the flow of all gases into the framework can increase the residence time and maximum abundance of a desired gas. Colored data points are obtained by averaging over 10 independent simulations (box dimensions 40 × 80). Circles corresponds to the points at which the framework is half-full of CO_2, *i.e.* where $\rho_{CO_2} = 0.5$. At the point shown by the square in (b), $\rho_{CO_2} \approx 0.9$. Curves are Arrhenius fits to the data, and have been extrapolated to lower temperature. The system sizes used in these simulations are correspond to a characteristic grain length of 27.2 nm; the characteristic times are longer for larger system sizes (see text).

4 Conclusions

We have studied a simple model of gas-framework dynamics inspired by experiment and parameterized using quantum mechanical data. For a set of three gas types whose hierarchy of mobilities in a crowded environment is the reverse of their hierarchy of framework-binding affinities, a gas (CO_2) that is essentially absent from the framework under equilibrium conditions can be captured under nonequilibrium conditions. To make precise predictions for specific experiments it may be necessary to relax several of the simplifying assumptions that we have made. For instance, we have neglected attractive molecule–molecule interactions, which at sufficiently low temperature may induce condensation or phase coexistence within the framework.[40,41] We have also considered the existence of only one kind of binding site, although in Mg-MOF-74 the displacement of CO_2 by H_2O may involve the passing of CO_2 from the primary binding site to a secondary one, through a low-energy exchange pathway[22,24,42,43] (note though that CO_2 binds almost as strongly to the secondary site as the primary one in Mg-MOF-74,[42] indicating that energy barriers for its removal from the framework are similar to those assumed here). Nonetheless, our results agree qualitatively with existing

experimental observations: water inhabits Mg-MOF-74 in preference to CO_2 in equilibrium;[15,24] CO_2 can be resident within the Mg-MOF-74 for some considerable time away from equilibrium;[24] and narrower pores lead to better gas-capture selectivity.[32–35] The nonequilibrium 'filtration' mechanism seen in Fig. 2 and 3 provides a possible microscopic explanation for this latter phenomenon. We believe that this demonstration will provide insight into the nonequilibrium aspects of gas capture and help experimentalists to choose protocols and conditions to perform gas capture away from equilibrium.

Acknowledgements

We thank Pieremanuele Canepa and Rebecca Siegelman for discussions, and Rebecca Siegelman and Jeff Martell for comments on the manuscript. JK was supported by the Center for Gas Separations Relevant to Clean Energy Technologies, an Energy Frontier Research Center funded by the U.S. Department of Energy, Office of Science, Basic Energy Sciences under Award number DE-SC0001015. DP and SW were partially supported by the same Center, and by the Office of Science, Office of Basic Energy Sciences of the U.S. Department of Energy. TP acknowledges support from the Batteries for Advanced Transportation Technologies program, administered by the Assistant Secretary for Energy Efficiency and Renewable Energy, Office of Vehicle Technologies of the U.S. Department of Energy under Contract DE-AC02-05CH11231. This work was done as part of a User Project at the Molecular Foundry at Lawrence Berkeley National Laboratory, supported by the Office of Science, Office of Basic Energy Sciences, of the U.S. Department of Energy under Contract No. DE-AC02-05CH11231. The simulations were performed at the compute cluster Vulcan, managed by the High Performance Computing Services Group, at Lawrence Berkeley National Laboratory.

References

1 R. K. Pachauri, M. Allen, V. Barros, J. Broome, W. Cramer, R. Christ, J. Church, L. Clarke, Q. Dahe and P. Dasgupta, *et al.*, *Climate Change 2014: Synthesis Report, Contribution of Working Groups I, II and III to the Fifth Assessment Report of the Intergovernmental Panel on Climate Change*, IPCC, Geneva, Switzerland, 2014, p. 151.
2 W. L. Queen, M. R. Hudson, E. D. Bloch, J. A. Mason, M. I. Gonzalez, J. S. Lee, D. Gygi, J. D. Howe, K. Lee, T. A. Darwish, M. James, V. K. Peterson, S. J. Teat, B. Smit, J. B. Neaton, J. R. Long and C. M. Brown, *Chem. Sci.*, 2014, **5**, 4569.
3 H. Furukawa, K. E. Cordova, M. O'Keeffe and O. M. Yaghi, *Science*, 2013, **341**, 1230444.
4 H. Li, M. Eddaoudi, M. O'Keeffe and O. M. Yaghi, *Nature*, 1999, **402**, 276.
5 S. R. Caskey, A. G. Wong-Foy and A. J. Matzger, *J. Am. Chem. Soc.*, 2008, **130**, 10870.
6 H. Wu, W. Zhou and T. Yildirim, *J. Am. Chem. Soc.*, 2009, **131**, 4995.
7 A. L. Dzubak, L.-C. Lin, J. Kim, J. A. Swisher, R. Poloni, S. N. Maximoff, B. Smit and L. Gagliardi, *Nat. Chem.*, 2012, **4**, 810.
8 D. Britt, H. Furukawa, B. Wang, T. G. Glover and O. M. Yaghi, *Proc. Natl. Acad. Sci. U. S. A.*, 2009, **106**, 20637.
9 K. Sumida, D. L. Rogow, J. A. Mason, T. M. McDonald, E. D. Bloch, Z. R. Herm, T.-H. Bae and J. R. Long, *Chem. Rev.*, 2012, **112**, 724.
10 J.-R. Li, R. J. Kuppler and H.-C. Zhou, *Chem. Soc. Rev.*, 2009, **38**, 1477.
11 J.-R. Li, Y. Ma, M. C. McCarthy, J. Sculley, J. Yu, H.-K. Jeong, P. B. Balbuena and H.-C. Zhou, *Coord. Chem. Rev.*, 2011, **255**, 1791.
12 A. R. Millward and O. M. Yaghi, *J. Am. Chem. Soc.*, 2005, **127**, 17998.
13 W. Zhou, H. Wu and T. Yildirim, *J. Am. Chem. Soc.*, 2008, **130**, 15268.
14 J. Park, H. Kim, S. S. Han and Y. Jung, *J. Phys. Chem. Lett.*, 2012, **3**, 826.
15 J. A. Mason, T. M. McDonald, T.-H. Bae, J. E. Bachman, K. Sumida, J. J. Dutton, S. S. Kaye and J. R. Long, *J. Am. Chem. Soc.*, 2015, **137**, 4787.
16 T. M. McDonald, J. A. Mason, X. Kong, E. D. Bloch, D. Gygi, A. Dani, V. Crocellà, F. Giordanino, S. O. Odoh, W. S. Drisdell, B. Vlaisavljevich, A. L. Dzubak, R. Poloni, S. K. Schnell, N. Planas, K. Lee, T. Pascal, L. F. Wan, D. Prendergast, J. B. Neaton, B. Smit, J. B. Kortright, L. Gagliardi, S. Bordiga, J. A. Reimer and J. R. Long, *Nature*, 2015, **519**, 303.
17 J. Liu, P. K. Thallapally, B. P. McGrail, D. R. Brown and J. Liu, *Chem. Soc. Rev.*, 2012, **41**, 2308.
18 K. Lee, J. D. Howe, L.-C. Lin, B. Smit and J. B. Neaton, *Chem. Mater.*, 2015, **27**, 668.
19 J. A. Mason, K. Sumida, Z. R. Herm, R. Krishna and J. R. Long, *Energy Environ. Sci.*, 2011, **4**, 3030.
20 L. Valenzano, B. Civalleri, S. Chavan, G. T. Palomino, C. O. Areán and S. Bordiga, *J. Phys. Chem. C*, 2010, **114**, 11185.
21 Z. Bao, L. Yu, Q. Ren, X. Lu and S. Deng, *J. Colloid Interface Sci.*, 2011, **353**, 549.
22 P. Canepa, N. Nijem, Y. J. Chabal and T. Thonhauser, *Phys. Rev. Lett.*, 2013, **110**, 026102.
23 P. Canepa, C. A. Arter, E. M. Conwill, D. H. Johnson, B. A. Shoemaker, K. Z. Soliman and T. Thonhauser, *J. Mater. Chem. A*, 2013, **1**, 13597.
24 K. Tan, S. Zuluaga, Q. Gong, Y. Gao, N. Nijem, J. Li, T. Thonhauser and Y. J. Chabal, *Chem. Mater.*, 2015, **27**, 2203.
25 X. Kong, E. Scott, W. Ding, J. A. Mason, J. R. Long and J. A. Reimer, *J. Am. Chem. Soc.*, 2012, **134**, 14341.
26 R. Krishna and J. M. van Baten, *J. Phys. Chem. C*, 2012, **116**, 23556.
27 A. I. Skoulidas and D. S. Sholl, *J. Phys. Chem. B*, 2005, **109**, 15760.
28 R. Babarao and J. Jiang, *Langmuir*, 2008, **24**, 5474.
29 T. C. Drage, C. E. Snape, L. A. Stevens, J. Wood, J. Wang, A. I. Cooper, R. Dawson, X. Guo, C. Satterley and R. Irons, *J. Mater. Chem.*, 2012, **22**, 2815.

30 G. Li, P. Xiao, P. Webley, J. Zhang, R. Singh and M. Marshall, *Adsorption*, 2008, **14**, 415.
31 A. C. Kizzie, A. G. Wong-Foy and A. J. Matzger, *Langmuir*, 2011, **27**, 6368.
32 P. Nugent, Y. Belmabkhout, S. D. Burd, A. J. Cairns, R. Luebke, K. Forrest, T. Pham, S. Ma, B. Space, L. Wojtas, M. Eddaoudi and M. J. Zaworotko, *Nature*, 2013, **495**, 80.
33 C. Y. Lee, Y.-S. Bae, N. C. Jeong, O. K. Farha, A. A. Sarjeant, C. L. Stern, P. Nickias, R. Q. Snurr, J. T. Hupp and S. T. Nguyen, *J. Am. Chem. Soc.*, 2011, **133**, 5228.
34 K. Li, D. H. Olson, J. Seidel, T. J. Emge, H. Gong, H. Zeng and J. Li, *J. Am. Chem. Soc.*, 2009, **131**, 10368.
35 D.-X. Xue, Y. Belmabkhout, O. Shekhah, H. Jiang, K. Adil, A. J. Cairns and M. Eddaoudi, *J. Am. Chem. Soc.*, 2015, **137**, 5034.
36 J. Liu, J. Tian, P. K. Thallapally and B. P. McGrail, *J. Phys. Chem. C*, 2012, **116**, 9575.
37 R. Poloni, K. Lee, R. F. Berger, B. Smit and J. B. Neaton, *J. Phys. Chem. Lett.*, 2014, **5**, 861.
38 B. Liu, Q. Yang, C. Xue, C. Zhong, B. Chen and B. Smit, *J. Phys. Chem. C*, 2008, **112**, 9854.
39 B. Liu and B. Smit, *Langmuir*, 2009, **25**, 5918.
40 E. Braun, J. J. Chen, S. K. Schnell, L.-C. Lin, J. A. Reimer and B. Smit, *Angew. Chem., Int. Ed.*, 2015, **54**, 14349.
41 N. Höft and J. Horbach, *J. Am. Chem. Soc.*, 2015, **137**, 10199.
42 M. G. Lopez, P. Canepa and T. Thonhauser, *J. Chem. Phys.*, 2013, **138**, 154704.
43 W. L. Queen, C. M. Brown, D. K. Britt, P. Zajdel, M. R. Hudson and O. M. Yaghi, *J. Phys. Chem. C*, 2011, **115**, 24915.

